Variations in runout of rock avalanches controlled by fragmentation, not basal friction

by Ø. T. Haug[1,2], M. Rosenau[1], M. Rudolf[1], K. Leever[1,3], and O. Oncken[1]

[1]GFZ German Research Centre for Geosciences, Helmholtz Centre Potsdam, Telegrafenberg, 14473 Potsdam, Germany.
[2]Njord center, Department of Geosciences, University of Oslo, PO Box 1048, 0316 Oslo, Nporway.
[3]Currently at: Van Hall Larenstein University of Applied Sciences, Larensteinselaan 26a, 6882 Velp, The Netherlands.

Correspondence: Matthias Rosenau (rosen@gfz-potsdam.de)

This manuscript has not yet undergone peer review.

Preprint DOI: 10.31223/osf.io/2ntdc

Please cite as:

Haug, Ø. T. , Rosenau, M., Rudolf, M., Leever, K. Oncken, O. (2020): Variations in runout of rock avalanches controlled by fragmentation, not basal friction, EarthArXiv, https://dx.doi.org/10.31223/osf.io/2ntdc

Variations in runout of rock avalanches controlled by fragmentation, not basal friction

Ø. T. Haug[1,2], M. Rosenau[1], M. Rudolf[1], K. Leever[1,3], and O. Oncken[1]

[1]GFZ German Research Centre for Geosciences, Helmholtz Centre Potsdam, Telegrafenberg, 14473 Potsdam, Germany.
[2]Njord center, Department of Geosciences, University of Oslo, PO Box 1048, 0316 Oslo, Norway.
[3]currently at: Van Hall Larenstein University of Applied Sciences, Larensteinselaan 26a, 6882 Velp, The Netherlands.

Correspondence: Matthias Rosenau (rosen@gfz-potsdam.de)

Abstract. Rock avalanches are large rockslides consisting of highly fragmented materials that display exceptionally long runouts, which are found to correlate with their volume. Such volume-dependent runouts are conventionally attributed to dynamic lowering of the effective basal friction. However, even for similar volumes, the runouts are seen to span several orders of magnitude suggesting additional controlling factors. Here, we perform analogue models of fragmenting rockslides and compare them to natural rock avalanches. We show that for a given low basal friction, the runout of rock avalanches varies over two orders of magnitude and is determined by their degree of fragmentation. The fragmentation is observed to cause spreading, but also to increased mechanical interactions between fragments. Consequently, the runout's dependence on fragmentation appears to be determined by the competition between spreading and internal friction. This shows that variation in degree of fragmentation can explain the large variation of runout of rock avalanches.

1 Introduction

With volumes larger than 10^6 m^3, and speeds reported at over 150 km/h (Campbell, 1989), the destructive power of rock avalanches is unprecedented. They are exceptional hazards produced when very large rockslides disintegrate during transport (Hungr et al., 2013). The travel distance of the deposit front, or runout, is an important measure for their hazard assessment (Vaunat and Leroueil, 2002) and is generally found to be longer than their fall height (Hsü, 1975). This suggests low effective basal frictions, which is usually attributed to a reduced normal stress at the base, for which various mechanisms have been proposed (e.g. Kent, 1966; Shreve, 1968; Hsü, 1975; Melosh, 1979; Campbell, 1989). For convenience, the reduction in basal friction can be considered through an effective coefficient of friction, μ_{eff}, which emerges naturally when considering energy conservation of the simple case of a rigid block of mass M sliding down a planar slope

$$MgH' = \mu_{eff} MgL' \Rightarrow \mu_{eff} = \frac{H'}{L'} \tag{1}$$

where H' and L' is the vertical and horizontal displacement of the block, respectively. Unlike a block, however, a rock avalanche may deform and spread. Additionally, field observations of the displacement of rock avalanches are often given by vertical (H) and horizontal (L) distance from the deposit's front to the top of the main scarp. The resulting ratio

$$\mu_{ap} = \frac{H}{L} \tag{2}$$

is known as the Heim's ratio (Heim, 1882, as cited in Hsü, 1975), or the apparent coefficient of friction (Manzella and Labiouse, 2012), and serves as a proxy for μ_{eff}.

One of the best established, but perhaps least understood observations of rock avalanches, is the dependence of the Heim's ratio on volume: rockslides below a size of approximately 10^6 m^3 all have a relatively constant Heim's ratio of $\sim$0.4-0.7, but for larger rockslides it decreases with volume, reaching values $<$0.1 for volumes larger than 10^9 m^3 (Lucas et al., 2014). This suggests a scale dependent mechanism of decreasing apparent friction with volume that is only relevant for large volumes (Davies and McSaveney, 1999). Whether the effective friction also depends on volume is uncertain, though analysis by Lucas et al. (2014) suggests that this is the case.

The uncertainty lies in the fact that the runout is defined by the front of the deposits, and therefore contains the combined effect of both translation and spreading of the rock mass. The additional travel distance caused by spreading can have a profound effect on the runout (Staron and Lajeunesse, 2009), especially if the effective basal friction is low. Though often not considered, the process of fragmentation can play a crucial role in the spreading of rock avalanches (Bowman et al., 2012). Firstly, one may expect that the finer the material, the more flow-like the behavior, allowing the rock mass to spread more easily (Locat et al., 2006). Secondly, models of fragmenting rockslides suggest that dynamic fragmentation actively increases the spreading (Bowman et al., 2012; De Blasio and Crosta, 2015). However, fragmentation has also been shown to consume energy (Haug et al., 2016; Zhao et al., 2017), potentially at a cost to the runout length. The effect of fragmentation on the spreading, and therefore on the final runout of rock avalanches remains largely unknown.

We perform analogue models of dynamically fragmenting rock avalanches (Figure 1). While we do not know its origin, we hypothesize that there exists some mechanism that causes a low, but constant effective coefficient of friction. This entails that any variation in Heim's ratio is the result of variations in the degree of fragmentation. We describe the dependence observed between the runout and the degree of fragmentation in the form of a scaling law. Finally, we compare our experimental results to a set of natural Data and discuss their relevance to natural systems. All data underlying this study as well as additional data will be published open access in Haug et al. (2020).

2 Methods

In the experiments, a block of height h and length l_0 (width = l_0) of rock analogue material is accelerated down a plate held at an angle of 45° to the horizontal (Figures 1). After 1 m of travel, the sample impacts a horizontal plate causing it to fragment. Once the sample has moved onto the horizontal plate, the fragmented material spreads and finally comes to rest. We expect the effective friction coefficient to always be larger than the apparent one, i.e. $\mu_{eff} > \mu_{ap}$. Since the apparent friction

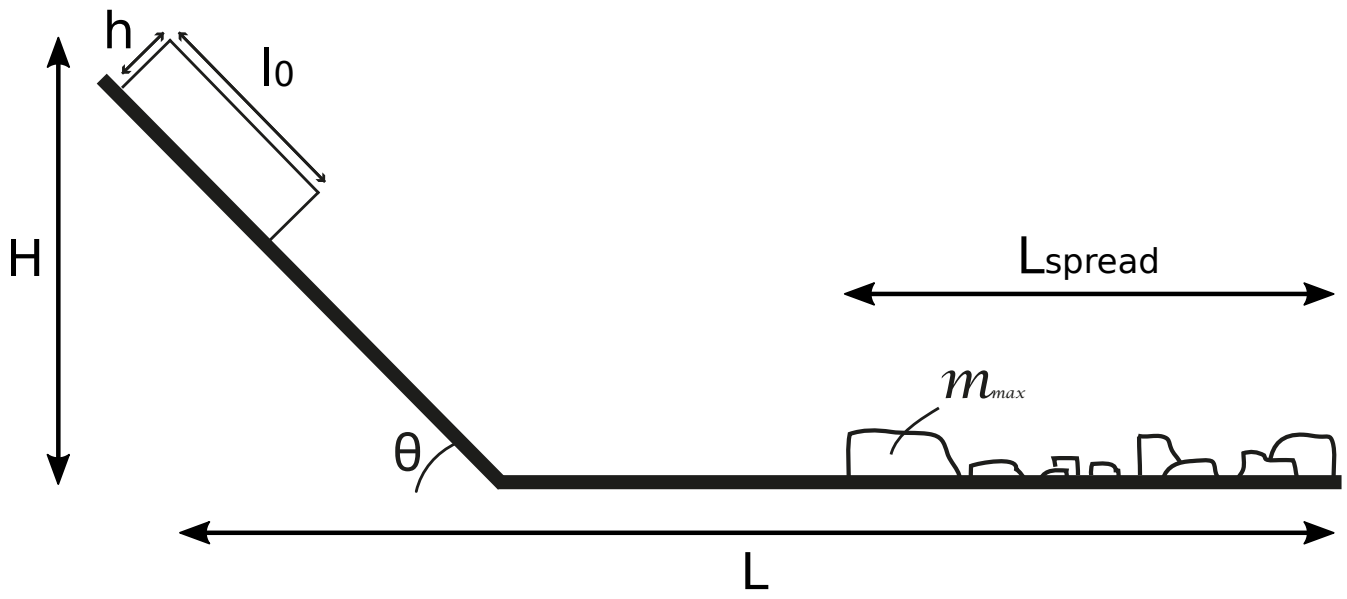

Figure 1. Sketch of the slope geometry of experiments and various length measurements (modified after Haug et al. (2016))

coefficient goes down to approximately 0.1 for rock avalanches (Lucas et al., 2014), we use glass as our substrate, which has a basal friction coefficient of 0.15 (Haug et al., 2016). The analogue rock material is cemented fluvial quartz sand. The sand is cemented by mixing it with water and gypsum or potato starch, and is left to set for 2 days (for gypsum cement) or heated for 15 minutes in a 900 W microwave (for potato starch cement). The cohesion of the material can be controlled by the type and the amount of cement added to the mixture, allowing control on the strength of the material over several orders of magnitude (see Haug et al., 2014, 2016, for details on the experimental setup).

The three main observables from the experiments are: (i) the degree of fragmentation (m_c), (ii) the Heim's ratio (H/L) and (iii) the normalized deposit length (L_{spread}/H). We characterize the degree of fragmentation through the total mass of the sample divided by the mass of the largest fragment ($m_c = M/m_{max}$), justification of which can be found in Haug et al. (2016). The front (and back) of the deposit is determined by the mass-weighted average position of the most distal 5 % of total mass. This defines a frontal rim which is a more robust runout estimate than using the foremost fragment position, used by Haug et al. (2016).

The experimental data presented here consists of the Heim's ratio and deposit lengths from two series of experiments with varying degree of fragmentation: (i) one series of experiments where the the thickness to length ratio ($h/l_0 = 0.033 - 0.49$) of the samples is varied while keeping the cohesion constant at $C = 14$ kPa. (ii) one series of experiments where the cohesion of the material ($C = 4 - 350$ kPa) is varied while keeping the thickness to length ratio constant at $h/l_0 = 0.13$. In both series of experiments, the fall height (H) is kept constant at 0.71 m. Interested readers are referred to Haug et al. (2016) for details on the effect of cohesion and geometry on the degree of fragmentation. Two additional experiments are studied in detail at the moment of fragmentation at high temporal resolution. For these experiments, the fragmentation of two samples with different

cohesions but equal geometry ($C = 4$ and 40 kPa, $h/l_0 = 0.13$) is considered. These two experiments have a fall height of 0.35 m, and data is captured by a camera with a frame rate of 500 Hz (see Haug et al., 2020, for movies of these experiments).

3 Observations

The Heim's ratio for experiments with different degrees of fragmentation (m_c) is plotted in Figure 2a. The two series of experiments follow the same trend (Haug et al., 2016), and no distinction is made between them in this figure. It shows that the Heim's ratio decreases rapidly for low to intermediate degrees of fragmentation, reaching a minimum at $m_c \approx 5$ of about 0.2. With further increase of fragmentation a gentle increase in the Heim's ratio is observed. A similar behavior is observed for the length of the deposits (Figure 2b), which increase until $m_c \approx 5$ before it decreases for higher values.

Figure 3 presents snapshots from the two additional experiments captured at a higher temporal resolution. As expected, the sample with the highest cohesion (Figure 3a) is observed to fragment less than the one with a lower cohesion (Figure 3b). However, these images also reveal that the fragments of the stronger sample spreads with limited interaction between the different fragments, whereas the fragments from the weaker sample collide and slide next to each other. This shows that a higher amount of internal deformation is experienced with increased fragmentation.

4 Interpretation and Discussion

4.1 Interpretation of experimental results

The rapidly decreasing Heims's ratio for $m_c < 5$ observed in Figure 2a is likely caused by the increased spreading with fragmentation (Figure 2b). A similar result was also obtained by previous analogue experiments (Bowman et al., 2012; Haug et al., 2016) as well as numerical models (De Blasio and Crosta, 2015; Zhao et al., 2017). However, here we show that the Heim's ratio is not simply decreasing with the degree of fragmentation, but that it displays an optimum for $m_c \approx 5$. Importantly, the lowest apparent basal friction, equivalent to the lowest Heim's ratio, is close to the implemented basal friction (i.e. friction coefficient of 0.15 between samples and glass). Therefore, all processes operating in our models (e.g. fragmentation, internal friction between fragments) tend to consume energy and thereby reduce runout from its optimum (Haug et al., 2016). Considering the increased internal deformation observed with the degree of fragmentation (Figure 3), the reduction of runout with $m_c > 5$ appears to be the result of the increased energy dissipation through internal friction. Consequently, the minimum of the Heim's ratio observed in Figure 2a is the result of a competition between spreading and internal friction.

This competition can be formalized into a scaling law by considering the conservation of energy (see Appendix A)

$$\frac{H}{L} = \mu \left(1 + \frac{\mu}{\sin\theta}\left(1 - \cos\theta\right) - \alpha log(m_c) - \beta e^{-m_c/\gamma}\right)^{-1} \tag{3}$$

where α, β, and γ are constants. This equation illustrates the competition between spreading ($\beta e^{-m_c/\gamma}$) and the increasing energy dissipation ($\alpha log(m_c)$) with m_c. A best fit of this function is presented in Figure 2a (blue line), where $\alpha = 0.12$, $\beta = 0.97$ and $\gamma = 1.7$. This suggests a strong effect of spreading for low degrees of fragmentation (i.e. $m_c < 5$), but with lesser

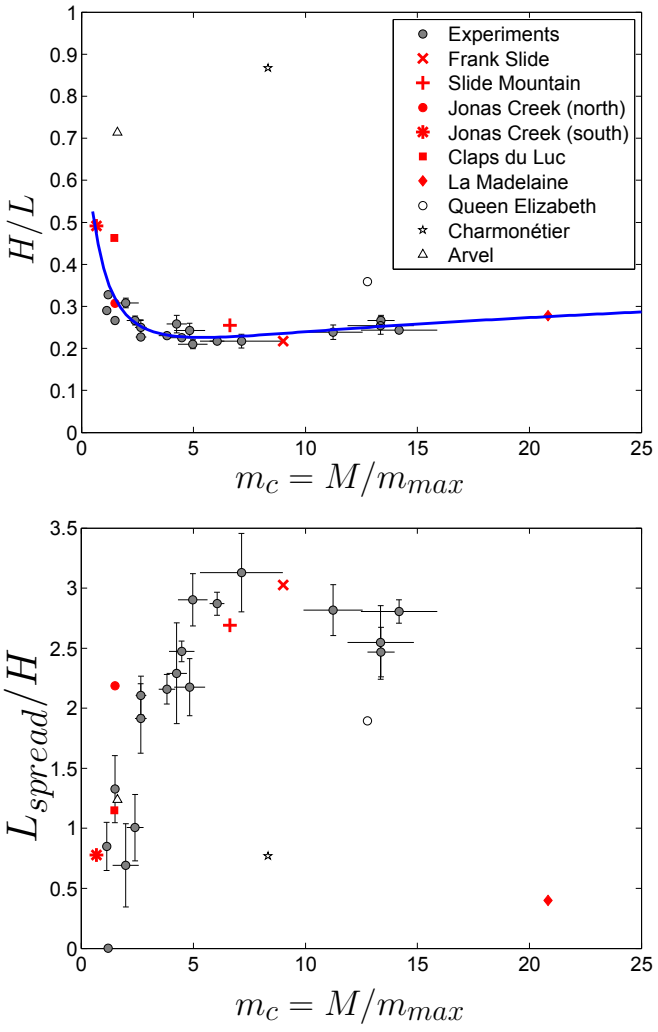

Figure 2. Heim's ratio and deposit length of experiments (this study) and natural rock avalanches (from Locat et al., 2006). (a) The Heim's ratio of the analogue experiments (gray) and from the rock avalanches (red = selected set, open = discarded). The blue line represents the best fit of Equation 3, with parameters $\alpha = 0.12$, $\beta = 0.97$ and $\gamma = 1.7$. (b) The deposit's lengths. In both panels, the gray circles represent the average value of a set of 4-15 experiments and the error bars give the standard error of the set. Data shown and a Matlab-script to plot them will be available in Haug et al. (2020).

effect at high degrees of fragmentation as the term $\beta e^{-m_c/\gamma}$ approaches zero. At high degrees of fragmentation, the energy dissipation related to fragmentation therefore becomes increasingly relevant.

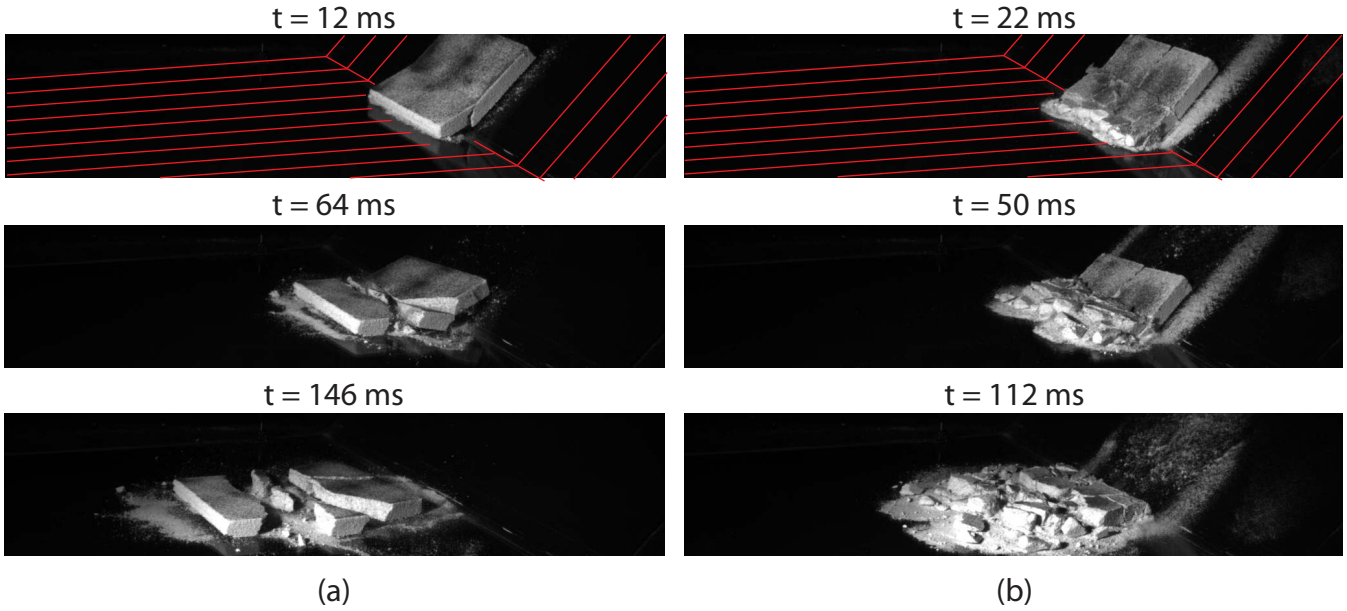

Figure 3. Snapshots from the experiments: (a) intermediate strength sample ($C = 40$ kPa) and (b) low strength sample ($C = 4$ kPa). The stronger sample (a) breaks apart into six large fragments with limited amount of fine material produced and move apart with little interaction after breaking. In contrast, the weaker sample fragments into many small pieces, with a large fraction of fine material, that interact more strongly. The red lines in the upper images indicate the geometry of the basal plates. The time given above each image reflects the time since first impact. The samples have dimensions 15x15x2 cm. Movies of the experiments will be available in Haug et al. (2020).

4.2 Comparison to a natural data set

We compare our experimental results (Figure 2) with data from nine rock avalanches reported by Locat et al. (2006), which show no clear volume dependence of runout. This makes this data set ideal to test whether a scale-independent process is operating besides dynamic basal weakening. However, not all the rock avalanches reported in (Locat et al., 2006) are comparable to our experimental setup by means of material properties and geometries (Figure 1). Based on slope geometry, the Queen Elizabeth slide is discarded because of its run-up on the opposite valley wall. Also discarded is the Charmonétier slide because of the sudden free fall stage at the end of its transport. Additionally, the Arvel slide was observed to bulldoze soft material in front of it, and such complexities are not considered in our models so this one is also neglected.

Figure 2 displays remarkably similar trends between the experimental and the selected natural data. The data points from Jonas Creek (north) and Clapse du Luc are observed to extend the trend from the experiments to higher Heim's ratio for low degrees of fragmentations: The agreement between these slides deposit lengths and the experimental ones (Figure 2b) suggests the extension of the trend in Heim's ratio is true. La Madelaine slide is observed to follow the trend of the experimental results of Heim's ratio to higher degrees of fragmentation (Figure 2a). If this point is indeed the continuation of the trend, its low spreading value (Figure 2b) suggests that the reduction of spreading indicated by the experiments for $m_c > 5$ continues for

even higher degrees of fragmentation. The Heim's ratios of the neglected slides are all, as expected, higher than the selected data set for their respective degrees of fragmentation, illustrating the importance of topography (e.g. opposite valley wall) and processes such as bulldozing.

The similarity seen between experimental and natural data suggests that the rock avalanches considered here have a close to constant effective friction of about 0.15. This implies that over a range of two orders of magnitude (from $2 \cdot 10^6$ to $90 \cdot 10^6$ m^3), the effective coefficient of friction of rock avalanches is independent of volume. Consequently, our results suggest that the variation seen in Heim's ratio for these rock avalanches are not caused by a different basal friction, but by differing degrees of fragmentation. This shows that fragmentation plays a governing role in the runout of rock avalanches and should be included in hazard assessments.

Data availability. The data for this paper will be available as an open access data publication (Haug et al., 2020).

Video supplement. Videos for this paper will be available as an open access data publication (Haug et al., 2020).

Appendix A: A mathematical description of the dependence on fragmentation of Heim's ratio

Generally, the conservation of energy of a sliding mass M requires that

$$MgH = \mu MgL_p + W \tag{A1}$$

where g is the gravitational acceleration, H is the vertical fall height, L_p is the entire travel path of the slide and W is the sum of any other energy dissipating terms. Here, we have assumed Coulomb friction at the base. For the geometry of our experimental setup (i.e. Figure 1), and also roughly for the set of selected rock avalanches, the L_p can be expressed in terms of the horizontal runout L as

$$L_p = L + L_s(1 - \cos\theta) - \frac{1}{2} l_0 \cos\theta - \frac{1}{2} L_{spread} \tag{A2}$$

where L_s is the length and θ the angle of the slope, and l_0 is the initial length of the slide. It is assumed that the additional travel length due to spreading is equal to half the deposit length (L_{spread}). Since l_0 is expected to be very small compared to the other terms, it is neglected in the further analysis. Inserting this expression into Equation A1 and solving for L gives

$$L = \frac{H}{\mu} - L_s(1 - \cos\theta) + \frac{1}{2} L_{spread}(\mu, \phi, m_c, W) - W(\mu, \phi, m_c) \tag{A3}$$

where it is emphasized that both L_{spread} and W is expected to be functions of the basal friction, μ, internal friction, ϕ, the degree of fragmentation, m_c, as well as a possible non-linear dependence between L_{spread} and W. With this expression for the runout, the Heim's ratio is

$$\frac{H}{L} = \mu \left(1 + \frac{\mu}{\sin\theta} (1 - \cos\theta) + \frac{L_{spread}(\mu, \phi, m_c, W)}{2H} - \frac{W(\mu, \phi, m_c, L_{spread})}{MgH} \right)^{-1} \tag{A4}$$

A direct determination of the two last terms in Equation A4 is difficult, however, the experimental work by Haug et al. (2016), suggests that W/Mgh can be described with a logarithmic function of m_c. Additionally, based on the shape of both the Heim' ratio and the L_{spread} plotted in Figure 2, it appears that it can be reasonably described by an exponential function of m_c. This leads to the approximation that

$$\frac{L_{spread}(\mu,\phi,m_c)}{2H} - \frac{W(\mu,\phi,m_c)}{MgH} = -\alpha log(m_c) - \beta e^{-m_c/\gamma} \tag{A5}$$

such that the Heim's ratio can be expressed as

$$\frac{H}{L} = \mu\left(1 + \frac{\mu}{\sin\theta}(1-\cos\theta) - \alpha log(m_c) - \beta e^{-m_c/\gamma}\right)^{-1} \tag{A6}$$

Author contributions. TEXT

Competing interests. TEXT

Disclaimer. TEXT

Acknowledgements. The authors would like to thank to Frank Neumann and Thomas Ziegenhagen for construction and technical assistance. The work has been supported by the Helmholtz Graduate Research School GEOSIM, the German Ministry for Education and Research (BMBF, FKZ03G0809A) and the Deutsche Forschungsgemeinschaft (DFG) through grant CRC 1114 "Scaling Cascades in Complex Systems" project B01. We thank Kirsten Elger and GFZ Data Services for publishing the data.

References

Bowman, E. T., Take, W. A., Rait, K. L., and Hann, C.: Physical models of rock avalanche spreading behaviour with dynamic fragmentation, Can. Geotech. J., 49, 460–476, https://doi.org/10.1139/t2012-007, 2012.

Campbell, C. S.: Self-lubrication for long runout landslides, The Journal of Geology, 97, 653–665, http://www.jstor.org/stable/10.2307/30062196, 1989.

Davies, T. R. and McSaveney, M. J.: Runout of dry granular avalanches, Can. Geotech. J., 36, 313–320, https://doi.org/10.1139/t98-108, 1999.

De Blasio, F. V. and Crosta, G. B.: Fragmentation and boosting of rock falls and rock avalanches, Geophysical Research Letters, 42, 8463–8470, https://doi.org/10.1002/2015GL064723, 2015.

Haug, Ø. T., Rosenau, M., Leever, K., and Oncken, O.: Modelling Fragmentation in Rock Avalanches, Landslide Science for a Safer Geo-Environment, 2, https://doi.org/10.1007/978-3-319-05050-8_16, 2014.

Haug, Ø. T., Rosenau, M., Leever, K., and Oncken, O.: On the Energy Budgets of Fragmenting Rockfalls and Rockslides: Insights from Experiments, Journal of Geophysical Research: Earth Surface, https://doi.org/10.1002/2014JF003406, http://doi.wiley.com/10.1002/2014JF003406, 2016.

Haug, Ø. T., Rosenau, M., Rudolf, M., Leever, K., and Oncken, O.: Laboratory model data from experiments on fragmenting analogue rock avalanches, https://doi.org/http://doi.org/10.5880/GFZ.2020.004, 2020.

Heim, A.: Der Bergsturz von Elm., Zeitschrift der Deutschen Geologischen Gesellschaft, pp. 74–115, 1882.

Hsü, K. J.: Catastrophic debris streams (sturzstroms) generated by rockfalls, Geological Society of America Bulletin, 86, 129–140, http://bulletin.geoscienceworld.org/content/86/1/129.short, 1975.

Hungr, O., Leroueil, S., and Picarelli, L.: The Varnes classification of landslide types, an update, Landslides, 11, 167–194, https://doi.org/10.1007/s10346-013-0436-y, 2013.

Kent, P. E.: The transport mechanism in catastrophic rock falls, The Journal of Geology, 74, 79–83, http://www.jstor.org/stable/10.2307/30075179, 1966.

Locat, P., Couture, R., Leroueil, S., Locat, J., and Jaboyedoff, M.: Fragmentation energy in rock avalanches, Canadian Geotechnical Journal, 43, 830–851, https://doi.org/10.1139/t06-045, 2006.

Lucas, A., Mangeney, A., and Ampuero, J. P.: Frictional velocity-weakening in landslides on Earth and on other planetary bodies., Nature communications, 5, 3417, https://doi.org/10.1038/ncomms4417, http://www.ncbi.nlm.nih.gov/pubmed/24595169, 2014.

Manzella, I. and Labiouse, V.: Empirical and analytical analyses of laboratory granular flows to investigate rock avalanche propagation, Landslides, https://doi.org/10.1007/s10346-011-0313-5, 2012.

Melosh, H. J.: Acoustic Fluidization : A New Geologic Process?, Journal of Geophysical Research, 84, 7513–7520, 1979.

Shreve, R. L.: Leakage and fluidization in air-layer lubricated avalanches, Geological Society of America Bulletin, 79, 653–658, https://doi.org/10.1130/0016-7606(1968)79, http://bulletin.geoscienceworld.org/content/79/5/653.short, 1968.

Staron, L. and Lajeunesse, E.: Understanding how volume affects the mobility of dry debris flows, Geophys. Res. Lett., 36, 2–5, https://doi.org/10.1029/2009GL038229, http://www.agu.org/pubs/crossref/2009/2009GL038229.shtml, 2009.

Vaunat, J. and Leroueil, S.: Analysis of Post-Failure Slope Movements within the Framework of Hazard and Risk Analysis, Natural Hazards, pp. 83–109, 2002.

Zhao, T., Crosta, G. B., Utili, S., and De Blasio, F. V.: Investigation of rock fragmentation during rockfalls and rock avalanches via 3D DEM analyses, Journal of Geophysical Research: Earth Surface, https://doi.org/10.1002/2016JF004060, http://doi.wiley.com/10.1002/2016JF004060, 2017.